DECTRIS
detecting the future

Application Note

PILATUS3 X CdTe detectors for in situ PXRD and operando XRD-CT experiments at synchrotron sources

Dr. Dubravka Šišak Jung, DECTRIS Ltd.

Introduction

One of the paramount concerns of the modern materials science is an environmentally friendly and cost-effective design of materials with advanced functionalities. While the common approach to the design of functional materials relies on establishing the structure-property relationship, the contemporary research focuses on the reaction mechanisms and on the behavior of materials in *in situ* and *operando* conditions. A good understanding of such dynamic systems correlates with a number of points in time at which interpretable data can be collected. Ideally, the data should not only allow for a reliable phase identification, but also provide information where in space the phase is. Although very challenging, these requirements were recognized and met at many high-energy beamlines. Exploiting the increased penetration depth, high flux, large area detectors and increased computation power, these beamlines have established new routines in materials science: *in situ* and *operando* XRD and XRD-CT studies. With the advent of PILATUS3 CdTe, these techniques were pushed one step further – towards better time and spatial resolution.

At the high-energy beamlines ID15A and ID31 at the European Synchrotron Radiation Facility, the PILATUS3 CdTe 2M is combined with a flexible experimental stage and smart data processing algorithms to enable two advanced techniques::

- *In situ* and real time Powder X-ray diffraction (PXRD)
- *Operando* X-Ray Diffraction Computed Tomography (XRD-CT)

DECTRIS
detecting the future

Application Note

In situ and real-time PXRD for monitoring mechanochemical reactions

One of the research fields that has largely benefitted from the advanced *in situ* and real-time PXRD measurements is mechanochemistry. As it relies on mechanical force to trigger chemical reactions between reactants in solid-state, mechanochemical milling is increasingly recognized as an environmentally friendly way to synthesize a variety of functional materials [1]. Although conceptually simple, its full implementation relies on several factors: good understanding of solid-state reactions, reliable indicators of the reaction end, and possibilities to scale up the production. Nowadays, ID15A and ID31 have set a new standard for investigation of milling reactions by using an in situ PXRD setup constructed around a specialized mill [2,3] and the PILATUS3 CdTe 2M detector.

This large-area detector is mounted on a translation stage, allowing users to optimize the angular coverage needed for the experiment. High quality of the collected data allows for crystal structure determination, even for weakly scattering materials exposed for only a couple of seconds. For example, the setup was used to synthesize and characterize a new polymorphic form of a pharmaceutical cocrystal (Figure 1) [5] and for identification of short-lived intermediates in the synthesis of a metal-organic framework [6].

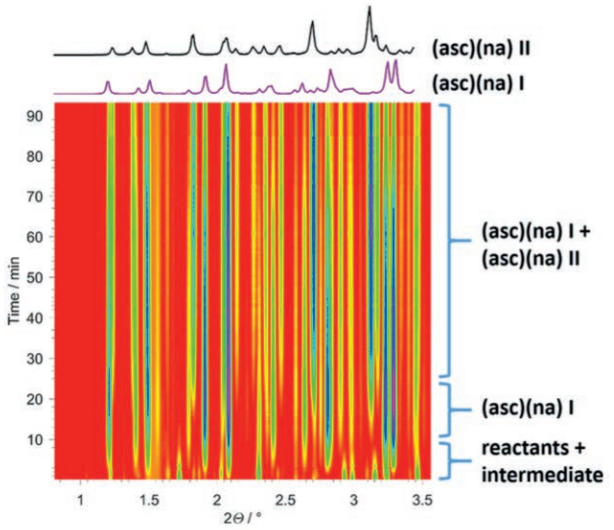

Figure 1. PXRD data obtained during time-resolved and in situ monitoring of mechanocemical reaction between vitamin C (asc) and nicotinamide (na) revealed a previously unknown polymorph of the cocrystal (asc)(na) II [5].

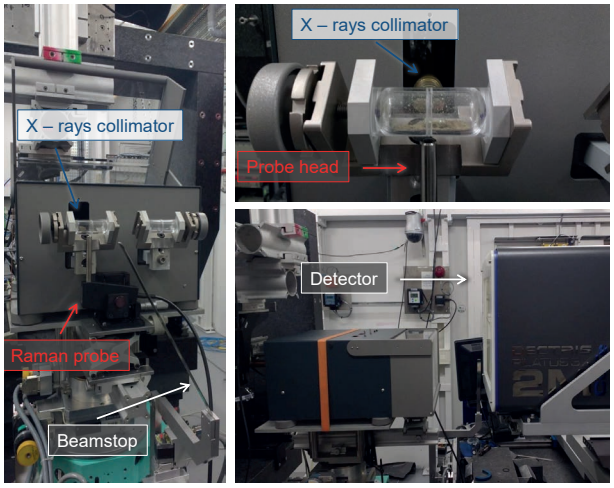

Figure 2. Tandem in situ monitoring: two complementary techniques, PXRD and Raman spectroscopy, are synchronized to give real-time information on molecular and crystal level of the investigated material.

The flexibility of the setup allows for the synchronisation of the PILATUS3 with a Raman spectrometer (Figure 2). Using the tandem PXRD-Raman *in situ* measurements, it is possible to facilitate the structural analysis during phase transitions, as well as to monitor migrations of hydrogen atoms during a solid-state reaction. Successful examples include synthesis of four new polymorphs of pharmaceutically-relevant cocrystals [7] and investigations of the selectivity of (co)crystallization processes [8,9]. Quantitative assessment and kinetic analysis of the mechanochemical reactions could be performed even on unknown crystal structures and short-lived intermediates.

Operando XRD-CT measurements for investigation of structure-activity relationships in catalytic and energy materials

Although the *in situ* setup added an additional dimension (time) to PXRD, the technique remains limited to systems where spatial distribution of reactants and products is not a critical parameter. In order to extend time-resolved X-ray diffraction to *operando* studies of complex systems, the technique had to be combined with computed tomography (CT). In this approach, the sample is illuminated with a pencil beam over a number of translational (T) and rotational (R) steps. The resulting 2D patterns are then integrated to give 1D patterns with d observation points and plotted

as a sinogram volume (TxRxd). Finally, the reconstructed real-space images are obtained by applying tomographic reconstruction algorithms to the sinogram data. By adjusting the number and value of translation and rotation steps, the measurement can be optimized to yield either a high spatial or a high temporal resolution.

Satisfying both, temporal and spatial resolution of the data, requires not only a synchrotron beam and a fast and large detector (Figure 3), but also a smart data collection strategy. By introducing the *interlaced XRD-CT* strategy, the ID15A users can perform subsequent XRD-CT scans with low spatial and high temporal resolution. In post experiment, these data can be combined to yield high spatial resolution XRD-CT data [11]. This enables fast-changing systems to be monitored at comparatively short timescales at modest resolution, or alternatively allows for improved spatial resolution if the system under study appears to be unchanging.

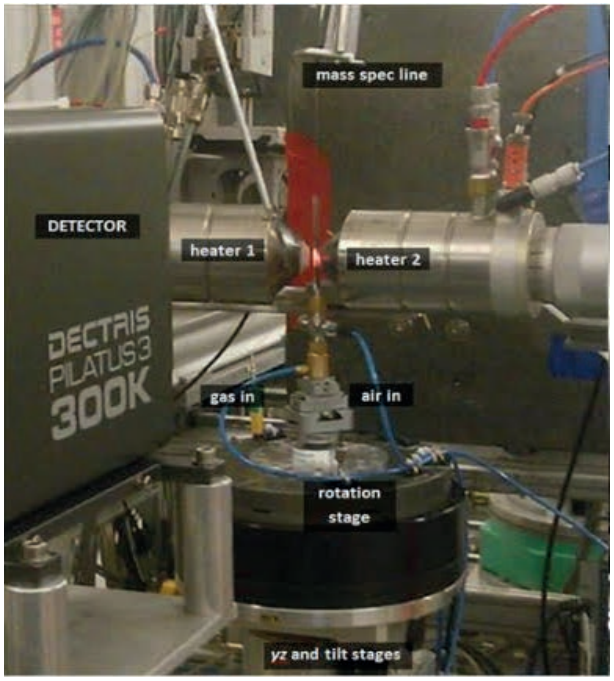

Figure 3. An example of an experimental setup used for XRD-CT at the ID15A beamline at the ESRF [12]. https://creativecommons.org/licenses/by/3.0/

In one of the first experiments, the setup was used for investigations of a membrane catalyst, used for conversion of methane to olefins. In order to improve its performance, operando XRD-CT was used to map the distribution of phases that are present in a cycle of catalyst membrane (Figure 5) [12].

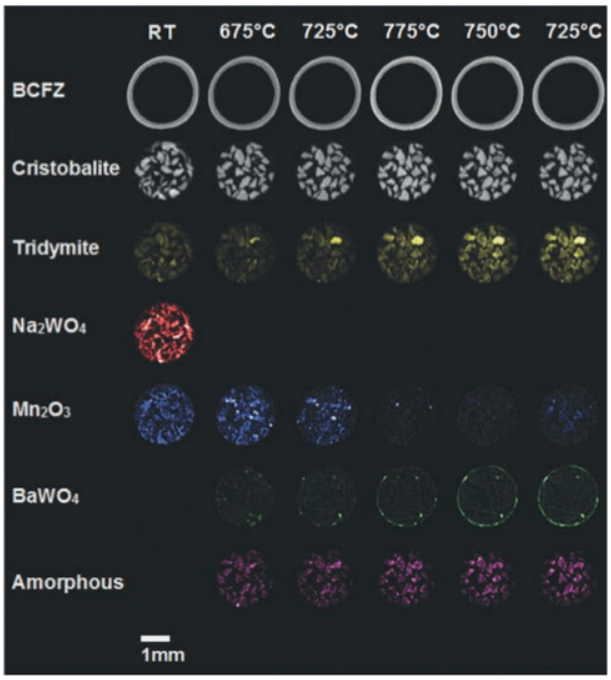

Figure 5.Cross-section through the membrane showing distribution of phases as a function of temperature increasing over time. The observation of the $BaWO_4$ correlates with the high and uncontrolled mobility of W at high temperatures, leading to the lower stability of the membrane and its deactivation of the membrane after many hours of operation by forming a layer at the membrane wall. The CT measurement was made with 130 translations over 180° in 1.8° steps covering a physical area of 2.6 x 2.6 mm. Reconstruction of these data yielded diffraction images with 130 x 130 pixels with 20 µm resolution. [12]. https://creativecommons.org/licenses/by/3.0/

Application Note

In another example, the XRD-CT setup was used for characterization of a new protonic ceramic fuel cell, used for conversion of chemical energy to electrical. Data on phase distribution maps throughout the working cycle of the cell (Figure 6) gave insights in mechanical robustness and thermal stability of the system, two important parameters for making the cell cost-effective [13].

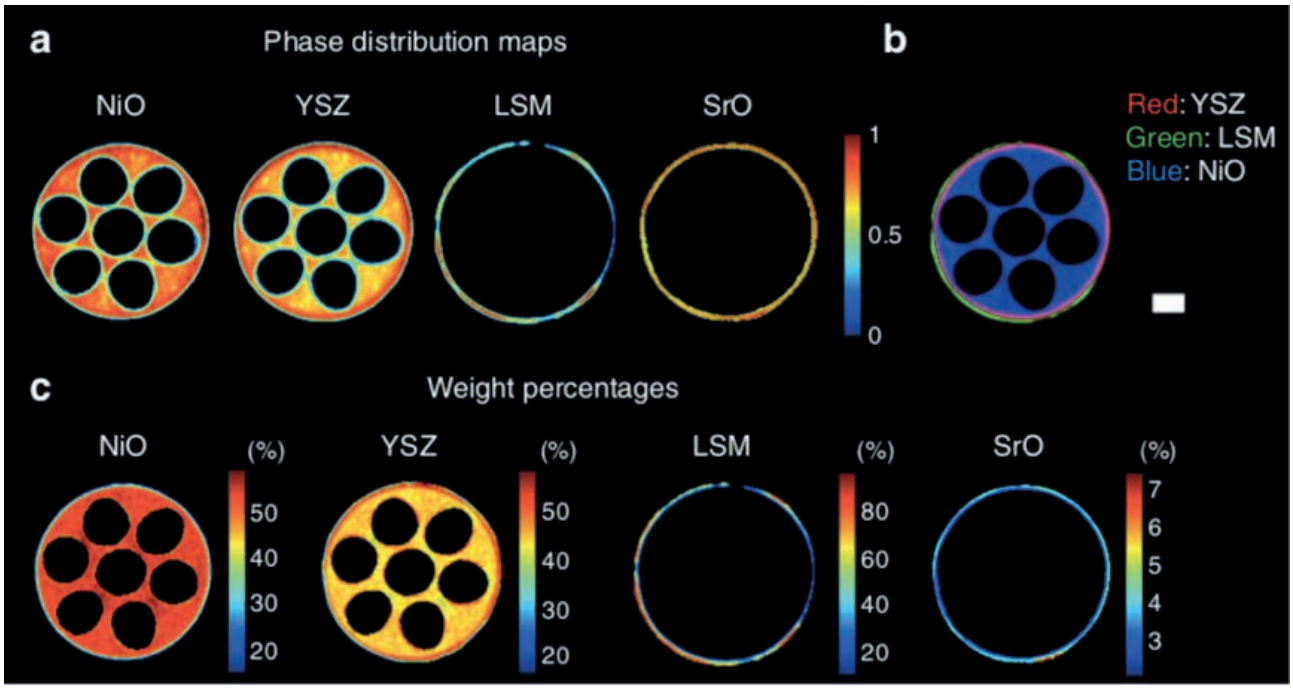

Figure 6. XRD-CT investigations on the mechanical robustness and structural integrity of the novel cell suggest excellent thermal cycling stability. (a) The phase distribution maps of NiO, YSZ, LSM and SrO as derived from the Rietveld analysis of the XRD-CT datasets (colour bar indicates intensity in arbitrary units). (b) red green blue (RGB) image showing the distribution of YSZ (red), LSM (green) and NiO (blue). (c) weight % of all crystalline phases present in the cell. The scale bar corresponds to 0.5 mm. The XRD-CT data were collected using a 90 keV beam, focused to a spot size of 40 µm x 20 µm. The total acquisition time per point was 20 ms and each XRD-CT scan lasted in total for 26 min [13]. https://creativecommons.org/licenses/by/4.0/

Application Note

DECTRIS
detecting the future

Technical specifications

PILATUS3 X CdTe detector series technical specifications

PILATUS3 X CdTe	300K	300K-W	1M	2M
Number of detector modules	1 × 3	3 × 1	2 × 5	3 × 8
Sensitive area: width × height [mm²]	83.8 × 106.5	253.7 × 33.5	168.7 × 179.4	253.7 × 288.8
Pixel size [µm²]	172 × 172			
Total number of pixels (horiz. × vert.)	487 × 619	1475 × 195	981 × 1043	1475 × 1679
Maximum count rate	5 x 10^6 counts/s/pixel (1.7 x 10^8 counts/s/mm²)			
Gap between modules (horiz. / vert.) [pixel], *plus 3 pixel horizontal gap on each module	–* / 17	7* / –	7* / 17	7* / 17
Inactive area [%]	6.1	1.6	7.8	8.5
Defective pixels	< 0.1%			
Maximum frame rate [Hz]	500	500	500	250
Readout time [ms]	0.95			
Point-spread function	1 pixel (FWHM)			
Threshold energy [keV]	8 - 40			
Counter depth	20 bits (1,048,576 counts)			
Power consumption [W]	30	30	165	250
Dimensions (WHD) [mm³]	158 × 193 × 262	280 × 62 × 296	265 × 286 × 455	384 × 424 × 456
Weight [kg]	7.5	7.0	25	46
Module cooling	Water cooled			
Electronics cooling	Water cooled		Air cooled	
External trigger/gating	5V TTL			

All specifications are subject to change without notice

Application Note

[1] References

[1] https://www.acs.org/content/acs/en/greenchemistry/principles/12-design-principles-of-green-engineering.html
[2] Halasz, I. *et al.* (2013) Nature Protocols 8(9), 1718-1729.
[3] Friščić, T. *et al.* (2013) Nature Chemistry 5, 66-73.
[4] https://www.insolidotech.com/
[5] Stolar, T. *et al.* (2017) Inorg. Chem. 56, 6599–6608.
[6] Stolar, T. et al. (2019) ACS Sustainable Chem. Eng. 7, 7102-7110.
[7] Lukin, S. *et al.* (2017) Chem. Eur. J. 23(56), 13941-13949.
[8] Lukin, S. *et al.* (2018) Cryst. Growth Des. 18, 1539-1547.
[9] Biliskov, N. *et al.* (2017) Chem. Eur. J. 23, 1-10.
[10] Lukin, S. *et al.* (2019) J. Am. Chem. Soc. 141, 1212-1216.
[11] Vamvakeros, A. et al. (2016) J. Appl. Cryst. 49, 485-496.
[12] Vamvakeros, A. *et al.* (2015) Chem. Commun. 51, 12752-12755.
[13] Li, T. *et al.* (2019) Nature Communications 10, 1497.